

Supporting Information

Harvesting mechanical energy induces piezoelectric polarization of MIL-100(Fe) for cocatalyst-free hydrogen production

Jie He, Ziran Yi, Qinqin Chen, Zhi Li, Jiayue Hu* and Mingshan Zhu*

Guangdong Key Laboratory of Environmental Pollution and Health, School of
Environment, Jinan University, Guangzhou 511443, P.R. China.

*Corresponding author email: M.Z. (zhumingshan@jnu.edu.cn)

Experimental Methods

Materials

Iron (III) nitrate nonahydrate ($\text{Fe}(\text{NO}_3)_3 \cdot 9\text{H}_2\text{O}$, 99.8%), 1,3,5-benzenetricarboxylic acid (98%), sodium hydroxide (NaOH, 99.9%), carbamazepine (CBZ, 99.8%), sodium sulfate (Na_2SO_4 , 99.8%), methanol (99.8%), ethanol (99.8%), 5, 5-dimethyl-1-pyrrolin-N-oxide (DMPO), KI (99.0%), $(\text{NH}_4)_6\text{Mo}_7\text{O}_{24} \cdot 4\text{H}_2\text{O}$ (99.0%), $\text{KHC}_8\text{H}_4\text{O}_4$ (99.8%) and other chemical agents were all analytical grades and purchased from Sigma Aldrich platform.

Characterization

Transmission Electron Microscope (TEM, JEOL 2010F) and scanning electron microscopy (SEM) were utilized to reveal the morphology, elemental mapping of as-synthesized MIL-100(Fe). X-ray diffraction (XRD, miniflex600, Japan) equipped with Cu-K α radiation was used to investigate the crystal structure of powder catalysts in the 2-theta degree range from 5 to 50. The optical absorption of MIL-100(Fe) was measured by UV-vis spectrometer (JASCO V-770). X-ray photoelectron spectroscopy (XPS) signals of MIL-100(Fe) were detected *via* Thermo Scientific K-Alpha XPS system (Thermo Fisher Scientific, UK). Piezoresponse force microscopy (PFM) with a scanning probe mode (Asylum Research, Nanoworld) was used to characterize the piezoelectric response of MIL-100(Fe) under direct current bias field. The nitrogen (N_2) adsorption Brunauer-Emmett-Teller (BET) method was applied to study the surface area of the sample using the Quantachrome Autosorb-IQ-MP adsorptometer.

Electrochemical characterizations were carried out using a three-electrode cell (CHI 760E, Shanghai Chenhua). The assembled electrodes (2 mg mL^{-1} water-ethanol solution of MIL-100(Fe) dropping with 20 μL Nafion) acted as the working electrode which worked on 1 \times 2 cm glass carbon electrode, while the Ag/AgCl electrode and the

Pt filament acted as reference electrode and counter electrode, respectively. Na_2SO_4 (pH=7) solution of 0.5 mol L^{-1} was used as electrolyte. Piezoelectric currents response and electrochemical impedance spectra (EIS) of MIL-100(Fe) were obtained under ultrasonic vibration of 40 kHz frequency and different mechanical power.

Synthesis of MIL-100(Fe)

MIL-100(Fe) was prepared following the procedures described in the literature.¹ Typically, $\text{Fe}(\text{NO}_3)_3 \cdot 9\text{H}_2\text{O}$ of 1.2 mmol and 1,3,5-benzenetricarboxylic acid of 1.0 mmol were dissolved in 5 mL deionized water. Then the resulting solution was stirred, transferred to a Teflon autoclave liner, and sealed to heat at 180 °C for 12 h. The obtained reddish-brown solid was collected by filtration and washed several times with deionized water and methanol. The synthesized MIL-100(Fe) was finally dried overnight at 60 °C in an oven.

Piezoelectric catalytic H_2 evolution and other catalysis processes

A 65 mL sealed Pyrex bottle worked as the reaction system to carry out H_2 evolution experiments. Firstly, 5 mg piezoelectric catalyst, 5 mL DI water with 50 μL methanol were added into the reaction bottle. Methanol could as a sacrificial agent to quench holes of catalysts. Then, the mixture was sealed and degassed air through N_2 for 20 min until the entire reaction system exhausts the air. A ultrasonic cleaner (KS-100DE, Kunshan) with frequency of 40 kHz and maximum power of 120 W was used to offer mechanical vibration. To avoid increasing of temperature induced by ultrasound, the circulating water were injected to keep the temperature at 25 ± 1 °C. The gaseous products in the system were analyzed by a gas chromatograph (GC-2014c, SHIMADZU, Japan) with a thermal conductivity detector (TCD) for H_2 detection. High purified N_2 (99.999%) and H_2 (99.999%) were used as carrier gas. The photo-catalytic H_2 evolution replaced ultrasonic vibration with light irradiation. A 300 W Xe lamp

(PLS-SXE300D, Beijing Perfectlight Technology Co., Ltd) acted as the light source, and the light intensity was 200 mW cm^{-2} .

The piezoelectric catalytic carbamazepine (CBZ) degradation were performed with or without scavenger by MIL-100(Fe). Typically, 30 mg MIL-100(Fe) was added into a beaker containing 30 mL CBZ (10 mg L^{-1}) aqueous solution, following the stirring of solution in darkness for 15 min to reach an adsorption–desorption equilibrium of reaction system. Then the beaker was put in the ultrasonic cleaner to provide mechanical force in the dark condition. The temperature was controlled at $25 \pm 1^\circ\text{C}$ via putting ice bags in the ultrasonic cleaner. At each regular time interval, 1 mL reaction sample was extracted and filtered with a $0.22 \mu\text{m}$ Teflon filter membrane for detection. The concentration of CBZ was analyzed through the high-performance liquid-chromatography (HPLC, Shimadzu LC-16 equipped with a diode array detector) using an acetonitrile/aqueous formic acid (60:40, v/v%) mixture as the mobile phase. In the quenching experiments, AgNO_3 (5 mmol L^{-1}) and TEMPO (5 mmol L^{-1}) were employed as the scavengers of e^- and $\text{O}_2^{\bullet-}$, respectively. Removal rates were calculated by the formulation: $\text{removal rate} = (1 - C_t/C_0)$, where C_t is the concentration of CBZ at time t , and C_0 is the initial concentration of CBZ. The generation of $\text{O}_2^{\bullet-}$ in the piezoelectric catalytic process was further investigated by the electron paramagnetic resonance (EPR, Bruker model EPR A300-10-12) technique at ambient temperature. DMPO was used to harvest $\text{O}_2^{\bullet-}$.

The piezoelectric catalytic hydrogen peroxide (H_2O_2) production by MIL-100(Fe) was also carried out in a 60 mL sealed Pyrex bottle. Briefly, The MIL-100(Fe) catalyst (1 g L^{-1}) was dispersed into a DI water solution (30 mL) and the bottle was sealed with a rubber septum cap with a gas inlet and outlet. Then the ultrasonic vibration was

applied by a ultrasonic cleaner (40 kHz, 96 W, Jielimei, Kunshan, China). The solution of 1 mL was extracted as sample data at fixed time to monitor H₂O₂ concentration. The concentration of H₂O₂ was measured according to the technology from the previous literature.² The freshly prepared potassium iodide reagent A of 1 mL (0.4 mol L⁻¹ KI, 0.05 mol L⁻¹ NaOH, 1.6 × 10⁻⁴ mol L⁻¹ (NH₄)₆Mo₇O₂₄·4H₂O) and 1 mL of reagent B (0.1 mol L⁻¹ KHC₈H₄O₄) were mixed with 1 mL solution sample of MIL-100(Fe) and stirred vigorously for 120 s. The absorbance at 350 nm was monitored using a UV-vis spectrophotometer for quantitative analyses of H₂O₂ concentration.

Supporting Figures

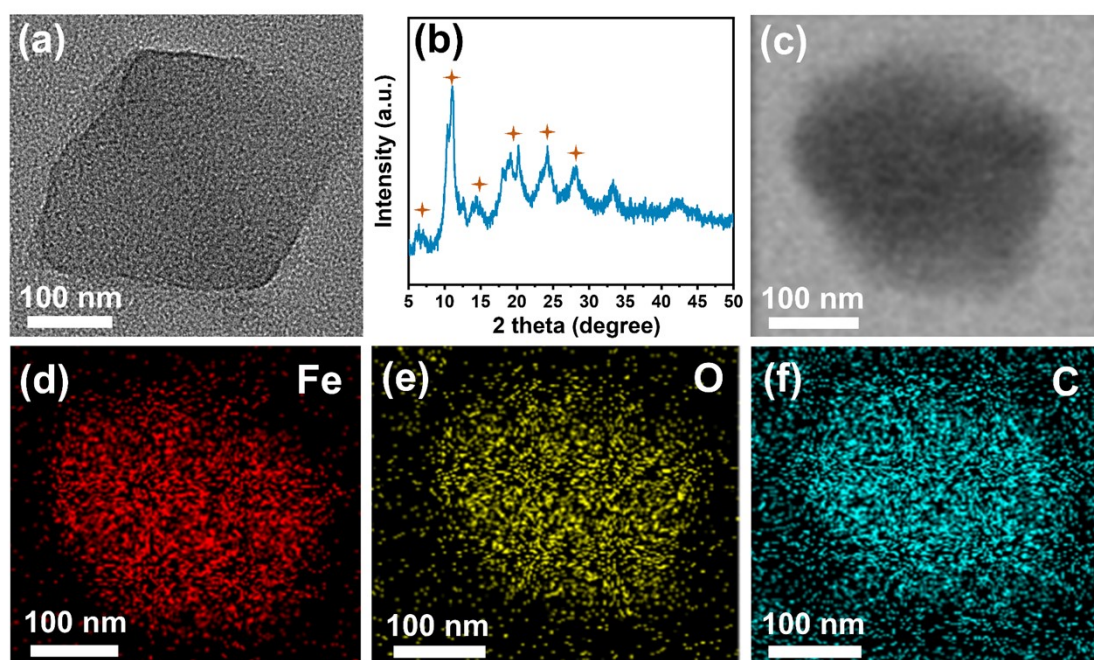


Fig. S1 (a) TEM image, (b) XRD pattern of MIL-100(Fe). (c-f) Scanning TEM images together with the corresponding elemental mappings of MIL-100(Fe).

Notes: Fig. S1a shows that the as-prepared MIL-100(Fe) possesses an octahedral morphology with the dimension of 50~200 nm. Fig. S1b exhibits XRD pattern of MIL-100(Fe) and presents good crystallinity, which is in agreement with reported diffraction patterns,^{3,4} and demonstrates the successful preparation of MIL-100(Fe). Additionally, the element mappings (Fig. S1c-f) reveal that Fe, O and C elements are uniformly distributed and there is no impurity in the MIL-100(Fe), proving the synthesis of Fe-based MOFs.

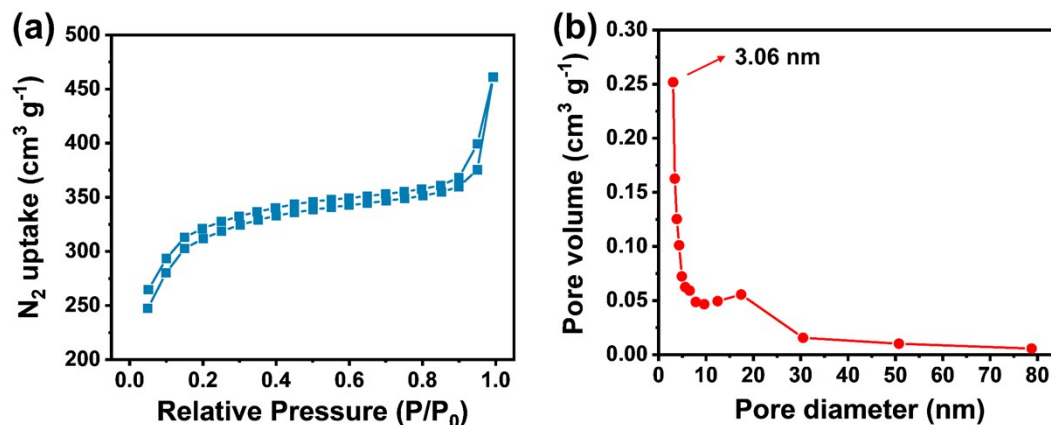


Fig. S2 (a) The N₂ adsorption-desorption isotherm at 77 K and (b) pore size distribution plot of as-synthesized MIL-100(Fe).

Notes: As depicted in the N₂ adsorption-desorption isotherms of Fig. S2a, MIL-100(Fe) possesses a hysteresis loop in the form of IV type isotherm, indicating that capillary condensation happens in the mesoporous structure.⁵ Such mesoporous MIL-100(Fe) has a large BET surface area of 1164.5 m² g⁻¹ with a small pore volume of 0.233 cm³ g⁻¹, and presents the pore diameter of 3.06 nm (Fig. S2b), which provides abundant catalytically active sites.

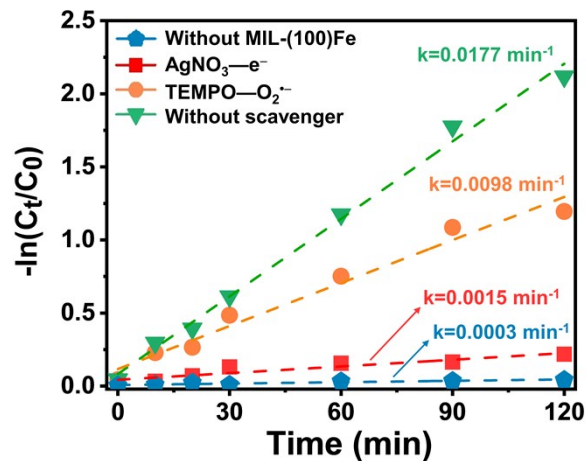


Fig. S3 The fit line plots of $-\ln(C_t/C_0)$ of the CBZ degradation rate in different systems.

Notes: We calculated the first-order kinetic rate constant of the CBZ degradation using MIL-100(Fe) to evaluate the performance of piezoelectric catalysis. The first-order kinetic rate constant (k) is calculated by following equations:

$$k = -\ln(C_t/C_0)/t$$

where C_t and C_0 are corresponding to residual concentrations and initial concentrations of CBZ, k is first-order rate constant and t is the reaction time. As shown in the Fig. S3, the k of MIL-100(Fe) for CBZ degradation without scavenger is 0.0177 min^{-1} , which is the highest among the four piezoelectric catalysis systems.

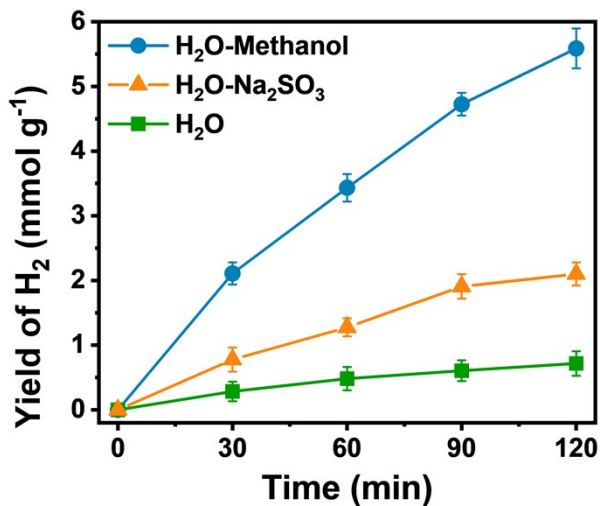


Fig. S4 The yield of H₂ evolution using MIL-100(Fe) with different electron donors under ultrasonic vibration (96 W power, 40 kHz vibration).

Notes: Fig. S4 exhibits that MIL-100(Fe) is able to achieve an upward trend of H₂ evolution under different systems *via* ultrasonic vibration. In the pure H₂O without electron donors, MIL-100(Fe) obtains about 0.73 mmol g⁻¹ H₂ within 2 h. After adding Na₂SO₃ and methanol as electron donors, the yield of H₂ increase to 2.13 mmol g⁻¹ and 5.60 mmol g⁻¹, indicating that electron donors, especially, the methanol can consume positive charges to provide more negative charges to improve HER performance.

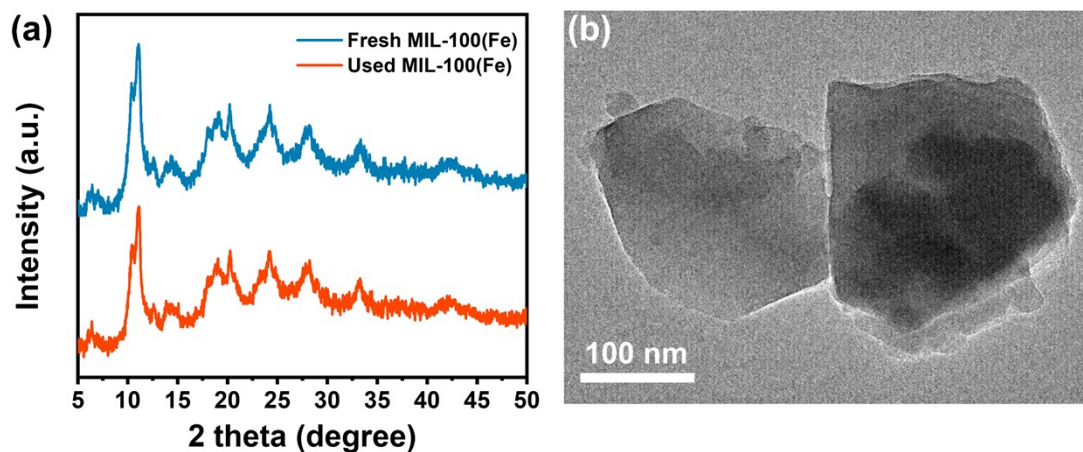


Fig. S5 (a) XRD patterns of MIL-100(Fe) before and after piezoelectric catalytic reaction. (b) TEM photograph of MIL-100(Fe) after piezoelectric reaction.

Notes: XRD patterns of MIL-100(Fe) before and after the 600-min piezoelectric reaction are similar without extra-generated secondary phases (Fig. S5a). TEM image of MIL-100(Fe) (Fig. S5b) also depicts that MIL-100(Fe) still maintains a stable octahedron shape after piezoelectric catalytic reaction. These results indicate an outstanding stability of structure and reusability of the as-prepared MIL-100(Fe) in piezoelectric catalytic process.

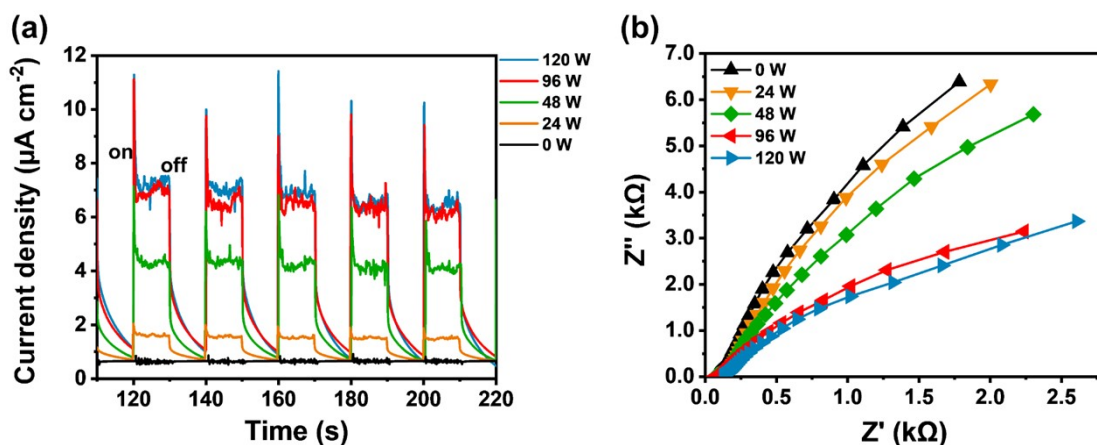


Fig. S6 (a) Transient piezoelectric current response and (b) electrochemical impedance spectroscopy of MIL-100(Fe) under different ultrasonic power.

Notes: The charges migration was tested through electrochemical measurements. The piezoelectric current response of MIL-100(Fe) is shown to confirm its piezoelectric charges separation (Fig. S6a). With ultrasonic stress on/off cycles, a transient and repeatable piezoelectric current response occurs in the MIL-100(Fe), and the current density improves along with boosting the ultrasound power until 96 W. The arc radius of EIS curve under the ultrasonic power of 120 W is the smallest, while there is no obvious difference of the radius between 96 W and 120 W power (Fig. S6b). Owing to a lower charge transfer resistance resulting in a higher mobility of q^- , a smaller arc radius is exhibited.⁶ Such phenomena are consistent with the piezoelectric H_2 evolution, revealing the ultimate mechanical pressure from 96 W power brings about the most efficient transfer of q^- on MIL-100(Fe).

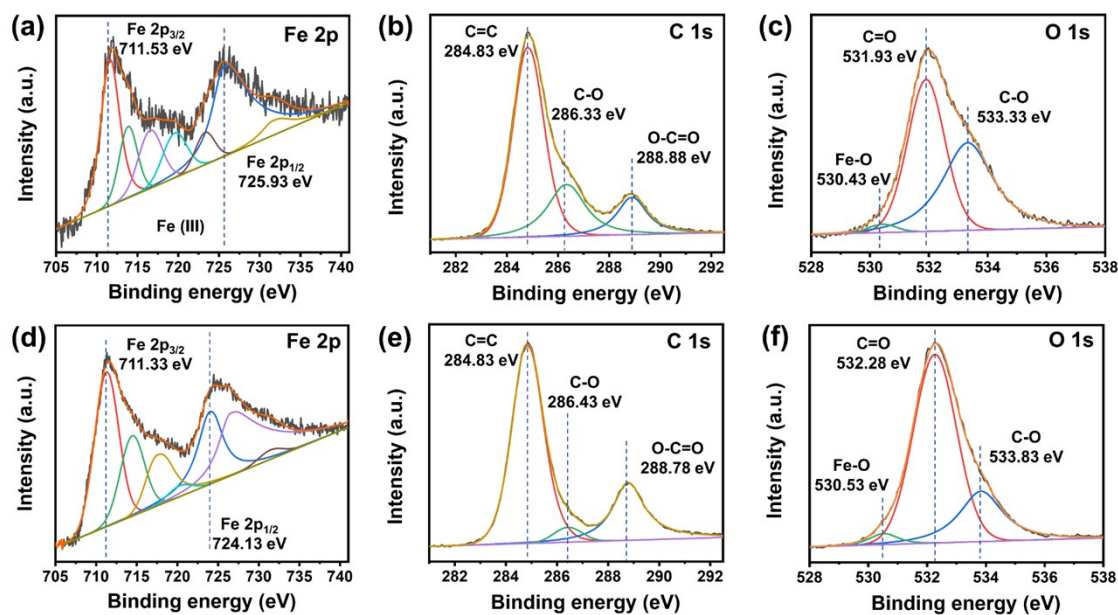


Fig. S7 XPS spectra of MIL-100(Fe) in (a) Fe 2p state, (b) C 1s state and (c) O 1s state before reaction. XPS spectra of MIL-100(Fe) in core level of (d) Fe 2p state, (e) C 1s state and (f) O 1s state after reaction.

Notes: In Fig. S7a, Fe 2p displays two peaks at 711.53 and 725.93 eV that are attributed to Fe 2p_{3/2} and Fe 2p_{1/2}, respectively, indicating the presence forms of Fe (III) in the MIL-100(Fe).⁷ For C 1s spectrum (Fig. S7b), three peaks are observed and assigned to the C=C of benzoic ring (284.83eV), the C-O bond (286.33 eV) and the carboxylate O-C=O (288.88 eV).⁸ The O 1s spectrum (Fig. S7c) also presents three peaks while the major peaks at 531.93 and 533.33 eV are corresponding to C=O and C-O bond, respectively, and the weak divided peak at 530.43 eV is belong to Fe-O bond.⁹

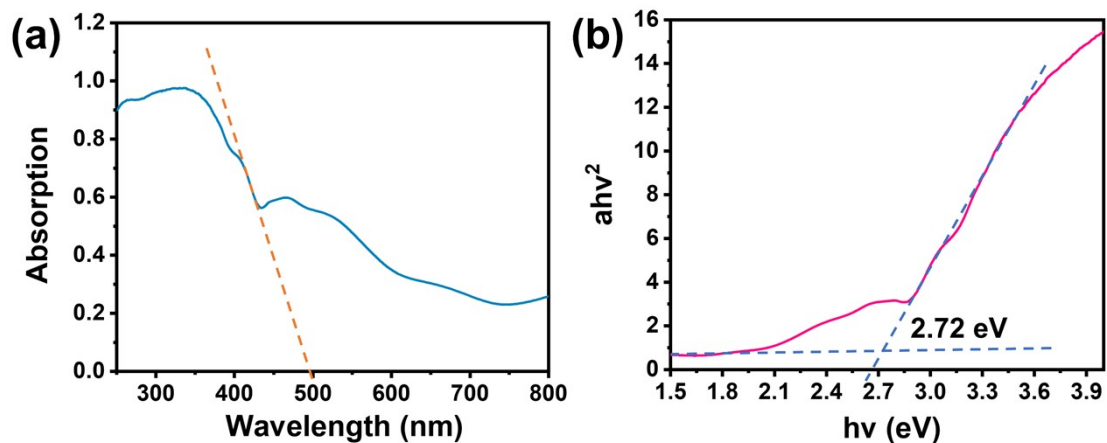


Fig. S8 (a) UV-Vis diffuse reflectance spectrum and (b) the corresponding Tauc's plots of MIL-100(Fe).

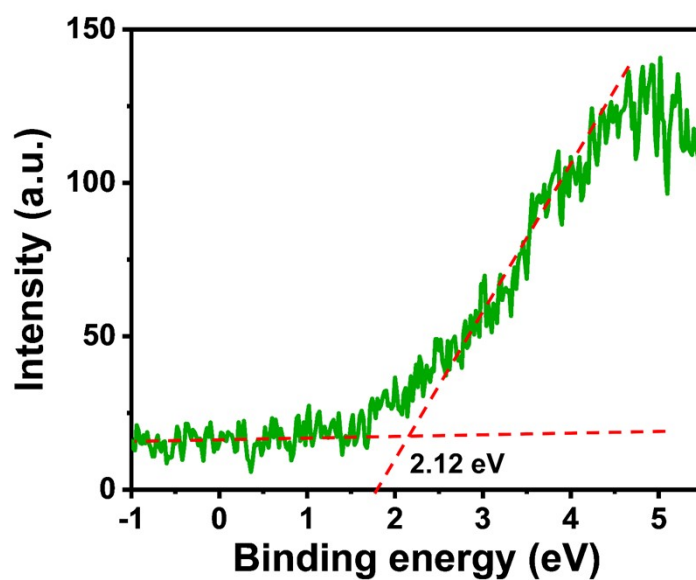


Fig. S9 The valence band (VB) spectrum of MIL-100(Fe) measured by XPS.

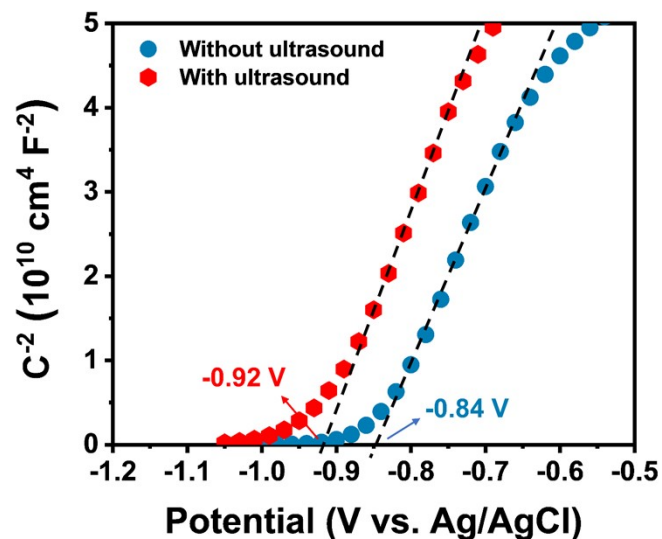


Fig. S10 The Mott-Schottky curves of MIL-100(Fe) with and without ultrasound.

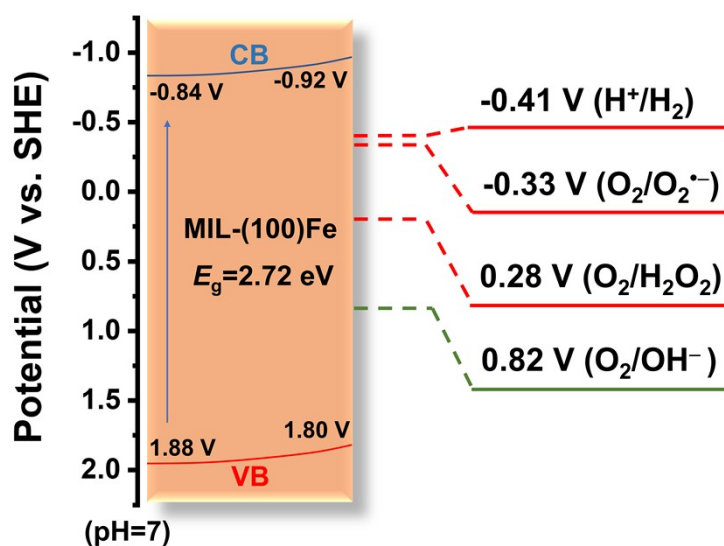


Fig. S11 Energy band tilting of the as-prepared MIL-100(Fe) and different potentials of redox reaction. (All the potentials are relative to the standard hydrogen electrode (SHE) at pH = 7).

Supporting References

1. D. Wang and Z. Li, *J. Catal.*, 2016, **342**, 151-157.
2. D. B. Rajamma, S. Anandan, N. S. M. Yusof, B. G. Pollet and M. Ashokkumar, *Ultrason. Sonochem.*, 2021, **72**, 105413.
3. G. Gnanasekaran, M. Sudhakaran, D. Kulmatova, J. Han, G. Arthanareeswaran, E. Jwa and Y. S. Mok, *Chemosphere*, 2021, **284**, 131244.
4. M. Nehra, N. Dilbaghi, N. K. Singhal, A. A. Hassan, K.-H. Kim and S. Kumar, *Environ. Res.*, 2019, **169**, 229-236.
5. M. Ahmad, S. Chen, F. Ye, X. Quan, S. Afzal, H. Yu and X. Zhao, *Appl. Catal. B-Environ.*, 2019, **245**, 428-438.
6. Y. Long, H. Xu, J. He, C. Li and M. Zhu, *Surf. Interfaces*, 2022, **31**, 102056.
7. L. Liu, Y. Liu, X. Wang, N. Hu, Y. Li, C. Li, Y. Meng and Y. An, *Appl. Surf. Sci.*, 2021, **561**, 149969.
8. J. Li, W. Huang, M. Wang, S. Xi, J. Meng, K. Zhao, J. Jin, W. Xu, Z. Wang and X. Liu, *ACS Energy Lett.*, 2018, **4**, 285-292.
9. Z. Zhang, Y. Muhammad, Y. Chen, S. J. Shah, Y. Peng, S. Shao, R. Wang, X. Li, H. Liu and Z. Zhao, *Chem. Eng. J.*, 2021, **426**, 131621.